Inorg. Chem. **2002**, *41*, 6662–6672

Paramagnetic ^{1}H NMR Spectrum of Nickel(II) Pseudoazurin: Investigation of the Active Site Structure and the Acid and Alkaline Transitions†

Christopher Dennison* and Katsuko Sato

Department of Chemistry, University of Newcastle upon Tyne, Newcastle upon Tyne NE1 7RU, U.K.

Received April 29, 2002

The paramagnetic ^{1}H NMR spectrum of Ni(II) pseudoazurin [(PA)Ni^{II}] possesses a number of resonances exhibiting sizable Fermi-contact shifts. These have been assigned to protons associated with the four ligating amino acids, His40, Cys78, His81, and Met86. The shifts experienced by the C$^{\gamma}$H protons of the axial Met86 ligand are unprecedented compared to other Ni(II)- and Co(II)-substituted cupredoxins (the C$^{\gamma 1}$H signal is found at 432.5 ppm at 25 °C). The large shift of protons of the axial Met86 ligand highlights a strong Ni(II)–S(Met) interaction in (PA)Ni^{II}. The paramagnetic ^{1}H NMR spectrum of (PA)Ni^{II} is altered by decreasing and increasing the pH value from 8.0. At acidic pH a number of the hyperfine-shifted resonances undergo limited changes in their chemical shift values. This effect is assigned to the surface His6 residue whose protonation results in a structural modification of the active site. Increasing the pH value from 8.0 has a more significant effect on the paramagnetic ^{1}H NMR spectrum of (PA)Ni^{II}, and the alkaline transition can now be assigned to two surface lysine residues close to the active site of the protein. The effect of altering pH on the ^{1}H NMR spectrum of Ni(II) pseudoazurin is smaller than that previously observed in the Cu(II) protein indicating more limited structural rearrangements at the non-native metal site.

Introduction

Pseudoazurin [(PA)Cu] is a type 1 blue copper protein (cupredoxin) which is found in denitrifying bacteria where it acts as the electron donor to a nitrite reductase (NiR).[1−3] The protein is made up of 8 β-strands which form 2 β-sheets giving an overall β-sandwich topology.[4−10] Additionally, pseudoazurin possesses two α-helices at its C-terminus. The single type 1 copper ion is buried approximately 5 Å from the protein surface and has a distorted tetrahedral geometry. The copper is strongly coordinated by the N$^{\delta}$ atoms of His40 and His81 and by the thiolate sulfur of Cys78 (see Figure 1). The copper ion is displaced from the plane of these three equatorial ligands by ∼0.4 Å in the direction of the thioether sulfur of the weak axial Met86 ligand (bond length 2.71 Å; see Figure 1). The His81 ligand of PACu protrudes through

* To whom correspondence should be addressed. E-mail: christopher.dennison@ncl.ac.uk. Tel: 44 191 222 7127. Fax: 44 191 222 6929.

† Abbreviations: (PA)Cu, pseudoazurin; (PA)Cu^{I}, reduced pseudoazurin; (PA)Cu^{II}, oxidized pseudoazurin; (PA)Ni^{II}, Ni(II)-substituted pseudoazurin; LMCT, ligand to metal charge transfer; LF, ligand field; UV/vis, ultraviolet/visible; NMR, nuclear magnetic resonance; SDS−PAGE, sodium dodecyl sulfate−polyacrylamide gel electrophoresis; 1D, one-dimensional; TOCSY, total correlation spectroscopy; WEFT, water-suppressed equilibrium Fourier transform; EPR, electron paramagnetic resonance; pH*, pH meter reading uncorrected for the deuterium isotope effect; HSE, Hahn spin−echo; CPMG, Carr−Purcell−Meiboom−Gill; Hepes, 4-(2-hydroxyethyl)piperazine-1-ethanesulfonic acid; Tris, tris(hydroxymethyl)aminomethane; HOMO, highest occupied molecular orbital; MWCO, molecular weight cutoff.

(1) Kakutani, T.; Watanabe, H.; Arima, K.; Beppu, T. *J. Biochem.* **1981**, *89*, 463−472.
(2) Liu, M. Y.; Liu, M. C.; Payne, W. J.; Legall, J. *J. Bacteriol.* **1986**, *166*, 604−608.
(3) Moir, J. W. B.; Baratta, D.; Richardson, D. J.; Ferguson, S. J. *Eur. J. Biochem.* **1993**, *212*, 377−385.
(4) Petratos, K.; Dauter, Z.; Wilson, K. S. *Acta Crystallogr.* **1988**, *B44*, 628−636.
(5) Adman, E. T.; Turley, S.; Bramson, R.; Petratos, K.; Banner, D.; Tsernoglou, D.; Beppu, T.; Watanabe, H. *J. Biol. Chem.* **1989**, *264*, 87−99.
(6) Vakoufari, E.; Wilson, K. S.; Petratos, K. *FEBS Lett.* **1994**, *347*, 203−206.
(7) Inoue, T.; Kai, Y.; Harada, S.; Kasai, N.; Ohshiro, Y.; Suzuki, S.; Kohzuma, T.; Tobari, J. *Acta Crystallogr.* **1994**, *D50*, 317−328.
(8) Inoue, T.; Nishio, N.; Suzuki, S.; Kataoka, K.; Kohzuma, T.; Kai, Y. *J. Biol. Chem.* **1999**, *274*, 17845−17852.
(9) Williams, P. A.; Fülöp, V.; Leung, Y. C.; Chan, C.; Moir, J. W. B.; Howlett, G.; Ferguson, S. J.; Radford, S. E.; Hajdu, J. *Nat. Struct. Biol.* **1999**, *2*, 975−982.
(10) Thompson, G. S.; Leung, Y. C.; Ferguson, S. J.; Radford, S. E.; Redfield, C. *Protein Sci.* **2000**, *9*, 846−858.

10.1021/ic020303p CCC: $22.00
Published on Web 11/15/2002

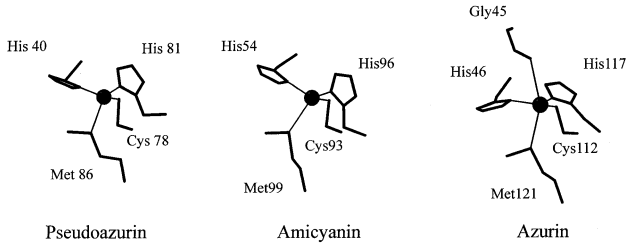

Figure 1. Representation of the active site of (PA)Cu^{II} from *A. cycloclastes*[8] (PDB accession code 1BQK), Cu(II) amicyanin from *P. versutus*[11] (PDB accession code 1ID2), and Cu(II) azurin from *P. aeruginosa*[12] (PDB accession code 4AZU) all drawn with MOLSCRIPT.[13] In all three structures the copper ion is indicated as a black sphere. The Cu(II)−S(Met) bond lengths are 2.71, 2.84, and 3.11 Å in (PA)Cu^{II}, Cu(II) amicyanin and Cu(II) azurin, respectively.

a region on the protein's surface made up of nonpolar amino acid residues. Surrounding this hydrophobic patch is a number of basic side chains which have been shown to be important for the interaction of PACu with its physiological partner.[14,15]

Type 1 copper sites possess unique spectroscopic properties in their cupric states as a consequence of their coordination geometry.[16,17] This includes an intense S(Cys) $\pi \rightarrow$ Cu(II) $d_{x^2-y^2}$ ligand-to-metal charge transfer (LMCT) transition at around 600 nm in their visible spectra ($\epsilon \sim 2000-6000$ M^{-1} cm^{-1}). In all cases, a second LMCT band [S(Cys) $\sigma \rightarrow$ Cu(II) $d_{x^2-y^2}$] at ∼450 nm is observed with its intensity varying in different type 1 sites.[16,18−20] The EPR spectra of type 1 sites have unusually small hyperfine coupling constants in the g_z region, which has been attributed to the highly covalent nature of the Cu−S(Cys) bond.[17] Subtle differences exist in the spectroscopic properties of cupredoxins and type 1 copper sites have been classified as either axial or rhombic. Type 1 axial sites have little absorption at around 450 nm in their visible spectra and have little difference between the g_x and g_y values in their EPR spectra. The cupredoxins azurin, plastocyanin, and amicyanin all have type 1 axial sites. Type 1 rhombic copper sites, including that found in (PA)Cu^{II}, have increased absorption at ∼450 nm and have a larger separation between their g_x and g_y values. A correlation has been proposed between the length of the Cu−S(Cys) bond, the ratio between the electronic absorptions at ∼450 and 600 nm, and the degree of rhombicity in the EPR spectra of type 1 copper centers.[18−20] A stronger axial interaction at a type 1 site (usually observed for type 1 rhombic centers) pulls the copper out of the Cys-containing plane, both decreasing the axial symmetry of the EPR spectrum and influencing the two Cys(S) → Cu(II) LMCT bands (this geometric change is accompanied by the site becoming more tetragonal[21−23]). The enhanced axial interaction has been associated with a rotation of the Cu $d_{x^2-y^2}$ HOMO which increases its σ and decreases the π interaction with the thiolate sulfur of the Cys ligand (there is also an increase in the Met sulfur contribution to the HOMO).[21,23]

Metal substitution has been widely used in the study of type 1 copper sites.[24−60] The X-ray structures of various metal

(11) Romero, A.; Nar, H.; Huber, R.; Messerschmidt, A.; Kalverda, A. P.; Canters, G. W.; Durley, R.; Mathews, F. S. *J. Mol. Biol.* **1994**, *236*, 1196.
(12) Nar, H.; Messerschmidt, A.; Huber, R.; van de Kamp, M.; Canters, G. W. *J. Mol. Biol*. **1991**, *221*, 765−772.
(13) Kraulis, P. J. *J. Appl. Crystallogr*. **1991**, *24*, 946−950.
(14) Kukimoto, M.; Nishiyama, M.; Ohnuki, T.; Turley, S.; Adman, E. T.; Horinouchi, S.; Beppu, T. *Protein Eng.* **1995**, *8*, 153−158.
(15) Kukimoto, M.; Nishiyama, M.; Tanokura, M.; Adman, E. T.; Horinouchi, S. *J. Biol. Chem*. **1996**, *271*, 13680−13683.
(16) Canters, G. W.; Gilardi, G. *FEBS Lett*. **1993**, *325*, 39−48.
(17) Solomon, E. I.; Penfield, K. W.; Gewirth, A. A.; Lowery, M. D.; Shadle, S. E.; Guckert, J. A.; LaCroix, L. B. *Inorg. Chim. Acta* **1996**, *243*, 67−78.
(18) Han, J.; Loehr, T. M.; Lu, Y.; Valentine, J. S.; Averill, B. A.; Sanders-Loehr, J. *J. Am. Chem. Soc*. **1993**, *115*, 4256−4263.
(19) Lu, Y.; LaCroix, L. B.; Lowery, M. D.; Solomon, E. I.; Bender, C. J.; Peisach, J.; Roe, J. A.; Gralla, E. B.; Valentine, J. S. *J. Am. Chem. Soc*. **1993**, *115*, 5907−5918.
(20) Andrew, C. R.; Yeom, H.; Valentine, J. S.; Karlsson, B. G.; Bonander, N.; van Pouderoyen, G.; Canters, G. W.; Loehr, T. M.; Sanders-Loehr, J. *J. Am. Chem. Soc*. **1994**, *116*, 11489−11498.
(21) LaCroix, L. B.; Shadle, S. E.; Wang, Y.; Averill, B. A.; Hedman, B.; Hodgson, K. O.; Solomon, E. I. *J. Am. Chem. Soc*. **1996**, *118*, 7755−7768.
(22) Pierloot, K.; De Kerpel, J. O. A.; Ryde, U.; Olsson, M. H. M.; Roos, B. O. *J. Am. Chem. Soc*. **1998**, *120*, 13156−13166.
(23) LaCroix, L. B.; Randall, D. W.; Nersissian, A. M.; Hoitink, C. W. G.; Canters, G. W.; Valentine, J. S.; Solomon, E. I. *J. Am. Chem. Soc*. **1998**, *120*, 9621−9631.
(24) McMillin, D. R.; Rosenberg, R. C.; Gray H. B. *Proc. Natl. Acad. Sci. U.S.A.* **1974**, *71*, 4760−4762.
(25) Solomon, E. I.; Rawlings, J.; McMillin, D. R.; Stephens, P. J.; Gray, H. B. *J. Am. Chem. Soc.* **1976**, *98*, 8046−8048.
(26) Tennent, D. L.; McMillin, D. R. *J. Am. Chem. Soc*. **1979**, *101*, 2307−2311.
(27) Ferris, N. S.; Woodruff, W. H.; Tennent, D. L.; McMillin, D. R. *Biochem. Biophys. Res. Commun*. **1979**, *88*, 288−296.
(28) Church, W. B.; Guss, J. M.; Potter, J. J.; Freeman, H. C. *J. Biol. Chem*. **1986**, *261*, 234−237.
(29) Suzuki, S.; Sakurai, T.; Shidara, S.; Iwasaki, H. *Inorg. Chem*. **1989**, *28*, 802−804.
(30) Di Bilio, A.; Chang, T. K.; Malmström, B. G.; Gray, H. B.; Karlsson, B. G.; Nordling, M.; Pascher, T.; Lundberg, L. G. *Inorg. Chim. Acta* **1992**, *198*−*200*, 145−148.
(31) Mizoguchi, T. J.; DiBilio, A. J.; Gray, H. B.; Richards, J. H. *J. Am. Chem. Soc*. **1992**, *114*, 10076−10078.
(32) Moratal, J. M.; Salgado, J.; Donaire, A.; Jiménez, H. R.; Castells, J.; Martínez-Ferrer, M. J. *Magn. Reson. Chem*. **1993**, *31*, S41−S46.
(33) Moratal, J. M.; Salgado, J.; Donaire, A.; Jiménez, H. R.; Castells, J. *Inorg. Chem*. **1993**, *32*, 3587−3588.
(34) Moratal, J. M.; Salgado, J.; Donaire, A.; Jiménez, H. R.; Castells, J. *J. Chem. Soc., Chem. Commun*. **1993**, 110−112.
(35) Strong, C.; Harrison, S. L.; Zeger, W. *Inorg. Chem*. **1994**, *33*, 606−608.
(36) Blackwell, K. A.; Anderson, B. F.; Baker, E. N. *Acta Crystallogr*. **1994**, *D50*, 263−270.
(37) Utschig, L. M.; Bryson, J. W.; O'Halloran, T. V. *Science* **1995**, *268*, 380−385.
(38) Salgado, J.; Jiménez, H. R.; Donaire, A.; Moratal, J. M. *Eur. J. Biochem*. **1995**, *231*, 358−369.
(39) Moratal, J. M.; Romero, A.; Salgado, J.; Perales-Alarcón, A.; Jiménez, H. R. *Eur. J. Biochem*. **1995**, *228*, 653−657.
(40) Piccioli, M.; Luchinat, C.; Mizoguchi, T. J.; Ramirez, B. E.; Gray, H. B.; Richards, J. H. *Inorg. Chem*. **1995**, *34*, 737−742.
(41) Tsai, L. C.; Sjölin, L.; Langer, V.; Bonander, N.; Karlsson, B. G.; Vänngård, T.; Hammann, C.; Nar, H. *Acta Crystallog*. **1995**, *D51*, 711−717.
(42) Danielsen, E.; Bauer, R.; Hemmingsen, L.; Andersen, M. L.; Bjerrum, M. J.; Butz, T.; Tröger, W.; Canters, G. W.; Hoitink, C. W. G.; Karlsson, G.; Hansson, O.; Messerschmidt, A. *J. Biol. Chem*. **1995**, *270*, 573−580.
(43) Utschig, L. M.; Wright, J. G.; Dieckmann, G.; Pecoraro, V.; O'Halloran, T. V. *Inorg. Chem*. **1995**, *34*, 2497−2498.
(44) McCleskey, T. M.; Mizoguchi, T. J.; Richards, J. H.; Gray, H. B. *Inorg. Chem*. **1996**, *35*, 3434−3435.
(45) Salgado, J.; Jiménez, H. R.; Moratal, J. M.; Kroes, S.; Warmerdam, G. C. M.; Canters, G. W. *Biochemistry* **1996**, *35*, 1810−1819.
(46) Jiménez, H. R.; Salgado, J.; Moratal, J. M.; Morgenstern-Badarau, I. *Inorg. Chem*. **1996**, *35*, 2737−2741.
(47) Vila, A. J.; Fernández, C. O. *J. Am. Chem. Soc*. **1996**, *118*, 7291−7298.

derivatives have been determined[28,36,39,41,48,61] and have shown that there is very little change at the active site as a consequence of metal replacement. The substitution of copper by Co(II) and Ni(II) leads to type 1 sites with distinct UV/vis spectroscopic properties which provide detailed structural information about the coordination geometry at the active site.[24−27,29−31,35,40,45,49,54,58] Paramagnetic NMR has been used to investigate Cu(II) cupredoxins[49,52,55,62−68] and also their Co(II) and Ni(II) derivatives.[32−34,38,40,45,47,49,52−58,60] The study of Cu(II) cupredoxins by paramagnetic ^{1}H NMR spectroscopy is hindered by the relatively slow electronic relaxation of this metal, which leads to quite severe broadening of the hyperfine-shifted resonances resulting in a number of these being too broad to be directly observed. In the case of pseudoazurin we have recently assigned the directly observed resonances in the paramagnetic ^{1}H NMR spectrum of the Cu(II) protein.[68] However, it was not possible to observe the C$^\beta$H protons of the Cys78 ligand in these studies due to the relaxation properties of this metal.[68] Substitution of Cu(II) by the faster relaxing paramagnetic metal ions Co(II) or Ni(II) in cupredoxins results in ^{1}H NMR spectra which possess sharper hyperfine-shifted signals, and subsequently all of the protons associated with the ligating amino acids can usually be assigned. These two complementary paramagnetic NMR approaches have been used to provide detailed information about the active site structures of several cupredoxins.[49,53,55,58]

Amino acid residues, whose pK_a values are in the accessible pH range, can have a significant effect on the reactivity and structure of cupredoxins. In certain reduced cupredoxins, including (PA)Cu^{I}, the exposed His ligand protonates,[6,69,70] which has a dramatic effect on the reduction potential[71−74] and reorganization energy[75,76] of the protein. The protonation of noncoordinated residues can also have a significant effect on the reactivity of cupredoxins. Well-studied examples are the exposed His35 of *P. aeruginosa* azurin[59] and the surface His6 of (PA)Cu.[68] Alkaline transitions have been observed in a number of cupredoxins including the phytocyanins[49,67] and pseudoazurin[77] and are thought to be caused by the deprotonation of surface Lys residues situated close to the active site. In (PA)Cu^{II} it has been found that the ionization of His6 (pK_a $\sim$ 6.4) and the alkaline transition (pK_a $\sim$ 10.3) both result in a structural change at the active site in which the copper ion moves away from the axial Met ligand toward the equatorial plane.[64,68]

In this study we have investigated Ni(II) pseudoazurin [(PA)Ni^{II}] using paramagnetic ^{1}H NMR spectroscopy. This is the first such investigation of a Ni(II) cupredoxin with a type 1 rhombic site. We have assigned the hyperfine-shifted resonances in the spectrum of this paramagnetic metalloprotein and have investigated the effect of the protonation of His6, and also the alkaline transition, on the structure of the Ni(II) site.

Experimental Section

Protein Isolation and Purification. The denitrifying bacterium *Achromobacter cycloclastes* was grown and (PA)Cu isolated and purified, as described previously.[68] The protein obtained has a A_{278}/A_{594} ratio of 1.4 and gave a single band on a SDS−PAGE gel.

Preparation of (PA)Ni^{II}. The native copper ion was removed from (PA)Cu by dialyzing the protein (100 μM) at 4 °C for 2 days against a solution containing 10 mM potassium cyanide in 100 mM Tris, pH 8.0. To ensure complete removal of copper, this procedure was repeated. The apoprotein was then dialyzed against 10 mM Tris, pH 8.0, to remove the cyanide from the protein solution, and finally against 10 mM Hepes, pH 8.0 (all at 4 °C). This procedure resulted in removal of 99% of the copper from (PA)Cu. To introduce Ni(II) into the active site the protein ($\sim$10 μM) was incubated at room temperature in a solution containing a 30-fold excess of $Ni(NO_3)_2 \cdot 6H_2O$ in 10 mM Hepes buffer at pH 8.0. The

(48) Bonander, N.; Vänngård, T.; Tsai, L. C.; Langer, V.; Nar, H.; Sjölin, L. *Proteins Struct. Funct. Genet*. **1997**, *27*, 385−394.
(49) Fernández, C. O.; Sannazzaro, A. I.; Vila, A. J. *Biochemistry* **1997**, *36*, 10566−10570.
(50) Utschig, L. M.; Baynard, T.; Strong, C.; O'Halloran, T. V. *Inorg. Chem*. **1997**, *36*, 2926−2927.
(51) Danielsen, E.; Kroes, S. J.; Canters, G. W.; Bauer, R.; Hemmingsen, L.; Singh, K.; Messerschmidt, A. *Eur. J. Biochem*. **1997**, *250*, 249−259.
(52) Vila, A. J.; Ramirez, B. E.; DiBilio, A. J.; Mizoguchi, T. J.; Richards, J. H.; Gray, H. B. *Inorg. Chem*. **1997**, *36*, 4567−4570.
(53) Donaire, A.; Salgado, J.; Moratal, J. M. *Biochemistry* **1998**, *37*, 8659−8673.
(54) Romero, C.; Moratal, J. M.; Donaire, A. *FEBS Lett*. **1998**, *440*, 93−98.
(55) Salgado, J.; Kroes, S. L.; Berg, A.; Moratal, J. M.; Canters, G. W. *J. Biol. Chem*. **1998**, *273*, 177−185.
(56) Fernández, C. O.; Sannazzaro, A. I.; Díaz, L. E.; Vila, A. J. *Inorg. Chim. Acta* **1998**, *273*, 367−371.
(57) Hannan, J. P.; Davy, S. L.; Moore, G. R.; Eady, R. R.; Andrew, C. R. *J. Biol. Inorg. Chem*. **1998**, *3*, 282−291.
(58) Salgado, J.; Kalverda, A. P.; Diederix, R. E. M.; Canters, G. W.; Moratal, J. M.; Lawler, A. T.; Dennison, C. *J. Biol. Inorg. Chem*. **1999**, *4*, 457−467.
(59) Kolczak, U.; Dennison, C.; Messerschmidt, A.; Canters, G. W. *Handbook of Metalloproteins*; John Wiley & Sons: Chichester, U.K., 2001; pp 1170−1194.
(60) Donaire, A.; Jiménez, B.; Moratal, J. M.; Hall, J. F.; Hasnain, S. S. *Biochemistry* **2001**, *40*, 837−846.
(61) Nar, H.; Huber, R.; Messerschmidt, A.; Filippou, A. C.; Barth, M.; Jaquinod, M.; van de Kamp, M.; Canters, G. W. *Eur. J. Biochem*. **1992**, *205*, 1123−1129.
(62) Kalverda, A. P.; Salgado, J.; Dennison, C.; Canters, G. W. *Biochemistry* **1996**, *35*, 3085−3092.
(63) Bertini, I.; Ciurli, S.; Dikiy, A.; Gasanov, R.; Luchinat, C.; Martini, G.; Safarov, N. *J. Am. Chem. Soc*. **1999**, *121*, 2037−2046.
(64) Dennison, C.; Kohzuma, T. *Inorg. Chem*. **1999**, *38*, 1491−1497.
(65) Bertini, I.; Fernández, C. O.; Karlsson, B. G.; Leckner, J.; Luchinat, C.; Malmström, B. G.; Nersissian, A. M.; Pierattelli, R.; Shipp, E.; Valentine, J. S.; Vila, A. J. *J. Am. Chem. Soc*. **2000**, *122*, 3701−3707.
(66) Bertini, I.; Ciurli, S.; Dikiy, A.; Fernandez, C. O.; Luchinat, C.; Safarov, N.; Shumilin, S.; Vila, A. J. *J. Am. Chem. Soc*. **2001**, *123*, 2405−2413.
(67) Dennison, C.; Lawler, A. T. *Biochemistry* **2001**, *40*, 3158−3166.
(68) Sato, K.; Dennison, C. *Biochemistry* **2002**, *41*, 120−130.
(69) Guss, J. M.; Harrowell, P. R.; Murata, M.; Norris, V. A.; Freeman, H. C. *J. Mol. Biol*. **1986**, *192*, 361−387.
(70) Zhu, Z.; Cunane, L. M.; Chen, Z. W.; Durley, R. C. E.; Mathews, F. S.; Davidson, V. L. *Biochemistry* **1998**, *37*, 17128−17136.
(71) Katoh, S.; Shiratori, I.; Takamiya, A. *J. Biochem*. **1962**, *51*, 32−40.
(72) Armstrong, F. A.; Hill, H. A. O.; Oliver, B. N.; Whitford, D. *J. Am. Chem. Soc*. **1985**, *107*, 1473−1476.
(73) Dennison, C.; Kohzuma, T.; McFarlane, W.; Suzuki, S.; Sykes, A. G. *Inorg. Chem*. **1994**, *33*, 3299−3305.
(74) Dennison, C.; Vijgenboom, E.; Hagen, W. R.; Canters, G. W. *J. Am. Chem. Soc*. **1996**, *118*, 7406−7407.
(75) Lommen, A.; Canters, G. W. *J. Biol. Chem*. **1990**, *265*, 2768−2774.
(76) Di Bilio, A. J.; Dennison, C.; Gray, H. B.; Ramirez, B. E.; Sykes, A. G.; Winkler, J. R. *J. Am. Chem. Soc*. **1998**, *120*, 7551−7556.
(77) Kohzuma, T.; Dennison, C.; McFarlane, W.; Nakashima, S.; Kitagawa, T.; Inoue, T.; Kai, Y.; Nishio, N.; Shidara, S.; Suzuki, S.; Sykes, A. G. *J. Biol. Chem*. **1995**, *270*, 25733−25738.

uptake of Ni(II) was monitored using UV/vis spectrophotometry [the Ni(II) protein has a visible λ_{max} at 420 nm] and was found to be complete under these conditions in approximately 5 days. The excess Ni(II) was removed by ultrafiltration (Amicon, 5 kDa MWCO membrane), and the sample was exchanged into 10 mM Hepes buffer, pH 8.0.

UV/Vis Spectrophotometry. UV/vis spectra were acquired at 25 °C on a Perkin-Elmer λ 35 UV/vis spectrophotometer with the protein in 10 mM Hepes buffer, pH 8.0.

Protein Samples for Paramagnetic ^{1}H NMR Studies. For the paramagnetic NMR experiments (PA)Ni^{II} samples were exchanged into 10 mM potassium phosphate in 99.9% D_2O or 90% H_2O/10% D_2O using centrifugal ultrafiltration units (Centricon 10, Amicon) or in a stirred cell (Amicon, 5 kDa MWCO membrane) and typically contained 4 mM protein. The pH values of protein solutions were measured using a narrow pH probe (Russell KCMAW11) with an Orion 420A pH meter. The pH of the sample was adjusted using NaOD or DCl in deuterated solutions and NaOH and HCl in H_2O solutions. The pH values quoted in deuterated solutions are uncorrected for the deuterium isotope effect and are indicated by pH*.

^{1}H NMR Spectroscopy. ^{1}H NMR spectra were acquired on either a JEOL Lambda 500 or a Bruker Avance 300 spectrometer at either 10 or 25 °C. All chemical shifts are quoted in parts per million (ppm) relative to water using the relationship $\delta_{HDO} = -0.012t + 5.11$ ppm, where t is the temperature in °C.[63] Diamagnetic 1D spectra were acquired using a standard one pulse sequence employing presaturation of the H_2O or HDO resonance during the relaxation delay with a spectral width of ca. 8 kHz. One-dimensional spectra for the assignment of singlet resonances were acquired using the Hahn spin−echo (HSE) [90°$_x$−τ−180°$_y$−τ−] (τ = 60 ms) and Carr−Purcell−Meiboom−Gill (CPMG) [90°$_x$−τ−(180°$_y$−2τ)$_n$−180°$_y$−τ] (n = 59, τ = 1 ms) pulse sequences. Two-dimensional TOCSY spectra of (PA)Ni^{II} were acquired with mixing times of 70 ms, using a spectral width of ca. 8 kHz with 2048 points for t_2 and 256−512 t_1 increments.

The super-WEFT sequence (d1−180°$_x$−τ−90°$_{x,y}$−acq, where d1 is the relaxation delay and acq the acquisition time)[78] was used to observe fast relaxing signals. Data were acquired with spectral widths of approximately 100 kHz and were processed using 20−50 Hz of exponential line broadening as apodization. Steady-state 1D NOE difference spectra were acquired at two different temperatures (10 and 25 °C) and in most cases at two different pH values (8.0 and 5.6), to eliminate any chance of spectral overlap, using the approach of Banci et al.[79]

The spin−lattice (T_1) relaxation times of the hyperfine shifted resonances were determined using an inversion−recovery experiment. For this the super-WEFT sequence was used with a total effective relaxation delay (d1 plus acq) ranging from 30 to 200 ms. The interpulse delay (τ) was varied between 0.1 ms and the total effective relaxation delay. An exponential fit of the plots of peak intensity against τ, for a particular proton, yielded its T_1 value. Peak widths were measured using spectra which had not undergone any baseline correction.

Assignment Strategy. To assign the signals in the paramagnetic ^{1}H NMR spectrum of (PA)Ni^{II} we have used an approach utilizing dipolar connectivities. This method requires a structural model, and for this we have used the crystal structure of (PA)Cu^{II} from *A. cycloclastes* (PDB accession code 1BQK[8]). Hydrogens were added to this structure using the program Insight II.

(78) Inubushi, T.; Becker, E. D. *J. Magn. Reson.* **1983**, *51*, 128−133.
(79) Banci, L.; Bertini, I.; Luchinat, C.; Piccioli, M.; Scozzafava, A.; Turano, P. *Inorg. Chem.* **1989**, *28*, 4650−4656.

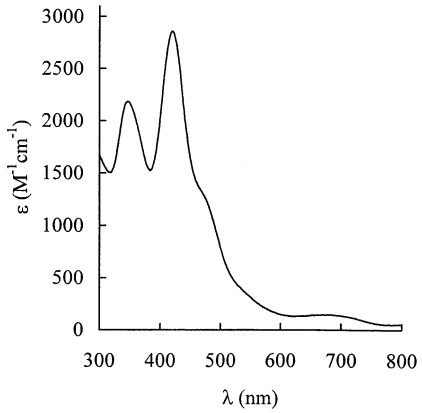

Figure 2. UV/vis absorption spectrum of (PA)Ni^{II} in 10 mM Hepes buffer at pH 8.0 (25 °C).

Table 1. Wavelengths (nm) and Intensities (ϵ, M^{-1} cm^{-1}) in Parentheses of the LMCT and LF Transitions in the UV/Vis Spectra of Ni(II)-Substituted Cupredoxins

pseudoazurin[a]	amicyanin[b]	azurin[c]	assignment[d]
346 (2180)	342 (1690)	354 (1350)	LMCT
420 (2850)	428 (2860)	440 (2900)	LMCT
480 (sh)[e]	495 (sh)	490 (sh)	[f]
550 (sh)		560 (150)	LF
680 (150)	690 (140)		LF

[a] This study. [b] Reference 58. [c] Reference 45. [d] As in ref 30. [e] Shoulder. [f] Not assigned in ref 30 but previously identified as an LMCT band.[26,81]

The NOE data were analyzed using eq 1 which is valid in the slow-motion limit,[80] where η_{ij} is the NOE observed for signal i upon irradiation of signal j, μ_0 is the magnetic permeability of a vacuum, $\hbar$ is Planck's constant (h) divided by 2π, γ_H is the magnetogyric ratio of the proton, τ_r is the rotational correlation time of the protein, r_{ij} is the distance between the protons i and j, and ρ_i is the longitudinal relaxation rate (T_1^{-1}) of proton i.

$$\eta_{ij} = -\left(\frac{\mu_0}{4\pi}\right)^2\left(\frac{\hbar^2\gamma_H{}^4\tau_r}{10r_{ij}{}^6\rho_i}\right) \quad (1)$$

Results

UV/Vis Spectrum of (PA)Ni^{II}. The UV/vis spectrum of (PA)Ni^{II} at pH 8.0 is shown in Figure 2 and is typical for a Ni(II)-substituted cupredoxin. The peak positions and intensities are listed in Table 1 along with the data for Ni(II) amicyanin and Ni(II) azurin. The intense absorption band at 420 nm (ϵ = 2850 M^{-1} cm^{-1}) is attributed[26,30,81] to a S(Cys) → Ni(II) LMCT transition. The less intense band at 346 nm also arises from an LMCT transition.[26,30,81] The spectrum contains a band at approximately 480 nm which appears as a shoulder on the much more intense 420 nm absorption, which is found in the spectra of other Ni(II)-substituted cupredoxins.[26,30,45,58,81] The ligand field (LF) transitions in (PA)Ni^{II} are typically not well resolved and are present as a shoulder at ∼550 nm and a broad band centered around 680 nm.

Effect of pH on the UV/Vis Spectrum of (PA)Ni^{II}. The effect of pH on the UV/vis spectrum of (PA)Ni^{II} was investigated in the pH range 4.0−11.2. Upon lowering

(80) Bertini, I.; Turano, P.; Vila, A. J. *Chem. Rev.* **1993**, *93*, 2833−2932.
(81) Lum, V.; Gray, H. B. *Isr. J. Chem.* **1981**, *21*, 23−25.

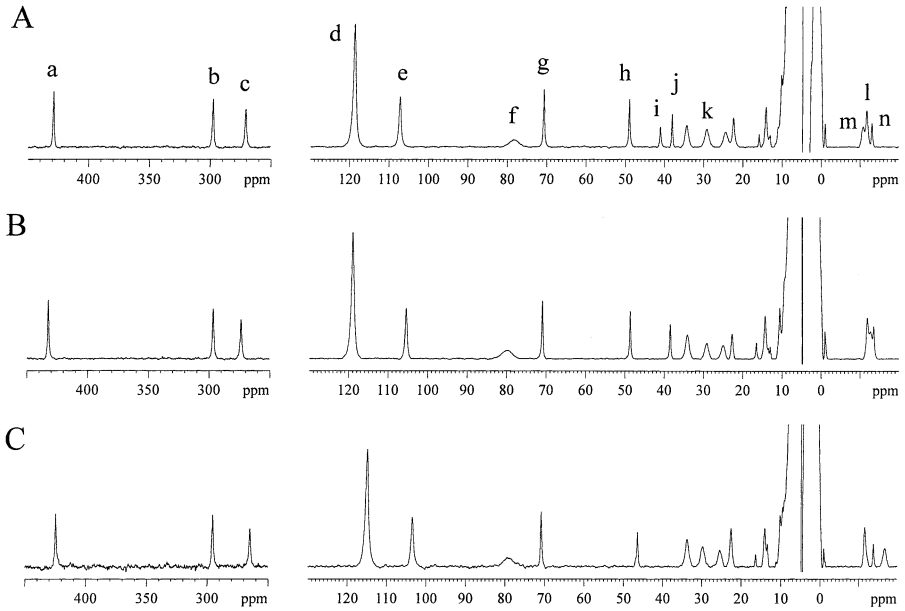

Figure 3. ^{1}H NMR spectra (300 MHz) of (PA)Ni^{II} (25 °C) in 10 mM phosphate buffer in 90% H_2O/10% D_2O at pH 5.1 (A), pH 8.0 (B), and pH 10.8 (C).

Table 2. Hyperfine-Shifted Resonances in the ^{1}H NMR Spectrum of (PA)Ni^{II} at 10 °C and pH 8.0[a]

resonance	δ (ppm)	T_1 (ms)	$\Delta\nu_{1/2}$ (Hz)	assignment
a	464.5 (432.5)[b]	3.2	330	Met86 C$^{\gamma 1}$H
b	315.5 (296.6)	3.9	440	Cys78 C$^{\beta 2}$H
c	293.7 (274.0)	2.8	760	Cys78 C$^{\beta 1}$H
d	128.0 (119.0)	8.5	370	Met86 C$^{\epsilon}$H$_3$
e	111.1 (105.4)	9.4	240	Met86 C$^{\gamma 2}$H
f	∼85 (80.0)	∼2	∼1600	His40 C$^{\epsilon 1}$H
g	75.2 (71.0)	35.6	80	His40 C$^{\delta 2}$H
h	51.1 (48.7)	39.6	70	His81 C$^{\delta 2}$H
i	43.2[c]	22.4[c]	70[c]	His81 N$^{\epsilon 2}$H
j	39.6 (38.5)	34.6	70	His40 N$^{\epsilon 2}$H
k	30.5 (29.2)	∼3	∼600	His40 C$^{\beta 1}$H
l	−14.5 (−11.9)	nd[d]	nd	[e]
m	−13.6 (−12.8)	11.6	nd	
n	−14.5 (−13.6)	38.1	nd	Cys78 C$^{\alpha}$H

[a] Data recorded at 300 MHz. Also included are the spin lattice (T_1) relaxation times, the observed chemical shifts, the peak widths ($\Delta\nu_{1/2}$), and the assignments that have been made. [b] Values in parentheses are those measured at 25 °C and pH 8.0. [c] Measured at pH 5.6 and 10 °C. [d] Not determined. [e] Slowly exchanging amide resonance.

the pH (from 8.0), almost no discernible alteration in the spectrum is observed. The sample becomes unstable at pH values below 5.0 and quite rapidly loses metal. Very little change is also seen in the pH range 8.0−10.3. At even higher pH values there are minor changes in the spectrum (the main difference being a slight shift in the position of the 346 nm peak). At pH 11.2 (PA)Ni^{II} is extremely unstable and all color disappears within a few minutes.

Paramagnetic ^{1}H NMR Spectrum of (PA)Ni^{II}. The paramagnetic ^{1}H NMR spectra of (PA)Ni^{II} in 90% H_2O/10% D_2O at pH 5.1, 8.0, and 10.8 are shown in Figure 3. The observed resonances in the spectrum of (PA)Ni^{II} are listed in Table 2 along with their spin−lattice (T_1) relaxation times and peak widths ($\Delta\nu_{1/2}$). The peaks labeled a−n have properties (hyperfine shifts, line widths, and T_1 values) which identify them as arising from protons associated with the ligating amino acid residues (see Figure 1). The two exchangeable resonances at around 40 ppm (peaks i and j) are characteristic of the imidazole N$^{\epsilon 2}$H protons of the two histidine ligands (His40 and His81). Peak j is observed in 90% H_2O/10% D_2O at pH 8.0 (see Figure 3B), whereas peak i is present only when the pH value of the sample is lowered further (below pH 5.8; see Figure 3A,B), indicating that it is in fast exchange with the bulk solvent at pH 8.0. This behavior is consistent with peak j belonging to the N$^{\epsilon 2}$H proton of the buried His40 ligand while peak i can be assigned to the N$^{\epsilon 2}$H proton of His81, which is more solvent exposed and is thus exchanging rapidly with bulk solvent (at pH 8.0). Two other exchangeable isotropically shifted resonances are observed (at 25 °C and pH 8.0) at 22.6 and −11.9 ppm (peak l). Both of these protons exchange quite slowly (over a few days) and thus are assigned to buried backbone amide protons quite close to the active site.

Selective irradiation of peak g leads to the identification of an NOE with peak j (see Figure 4B). The reverse connectivity is also observed upon the selective irradiation of peak j (data not shown). This indicates that peak g must also belong to the imidazole ring of His40. The long T_1 value of peak g, along with its relatively small line width, indicates that it cannot be situated too close to the paramagnetic metal center, and we therefore can assign it to the C$^{\delta 2}$H proton of His40 [the C$^{\delta 2}$H proton of His40 is 5.11 Å from the metal ion while the C$^{\epsilon 1}$H proton of this His ligand is only 3.16 Å away from the cupric ion in the (PA)Cu^{II} structure; see Figure 1]. Upon selective irradiation of the relatively sharp peak h at pH 5.6 (90% H_2O/10% D_2O), an NOE is observed to peak i (see Figure 4D). The reverse NOE is also observed upon selective irradiation of peak i (data not shown). The properties of peak h, and the observed NOEs, indicate that it belongs to the C$^{\delta 2}$H proton of His81. The histidine imidazole C$^{\epsilon 1}$H resonances are usually quite broad and have short T_1 times in the spectra of Ni(II) cupredoxins,[32,34,45,53,56,58] due to their proximity to the metal ion (vide supra). Peak f is characteristic (in terms of δ value and relaxation properties) of a coordinated His C$^{\epsilon 1}$H proton. Irradiation of this signal

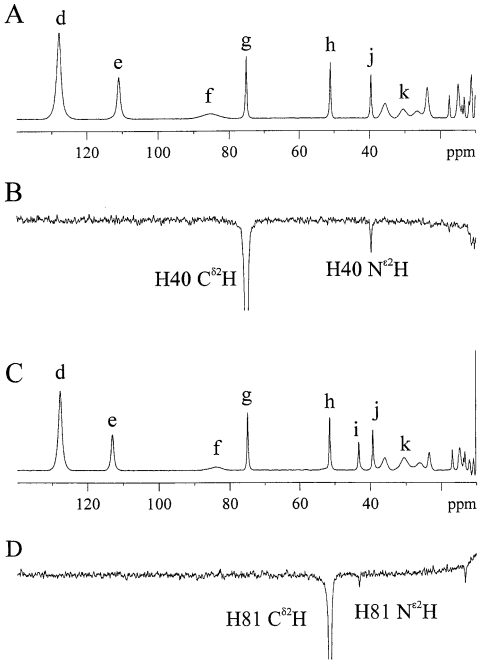

Figure 4. Reference (A and C) and difference (B and D) ^{1}H NMR spectra (300 MHz) of (PA)Ni^{II} corresponding to 1D NOE experiments performed in 10 mM phosphate buffer in 90% H_2O/10% D_2O (10 °C) at pH 8.0 (A and B) and pH 5.6 (C and D).

in both 90% H_2O/10% D_2O (at pH 8 and 5.6) and 99.9% D_2O did not result in the observation of NOEs to any other hyperfine shifted resonance and, in particular, not to the N$^{\epsilon 2}$H resonances of the two His ligands (peaks i and j, data not shown). The close proximity of peak f to the His40 C$^{\delta 2}$H resonance (peak g) in the spectrum of (PA)Ni^{II} results in a large off-resonance effect at signal g (and also at peak j) in the 1D NOE difference experiments in which peak f is irradiated which would prevent the observation of any NOE between peaks f and j. We therefore tentatively assign peak f as the His40 C$^{\epsilon 1}$H resonance. The three quite broad peaks in the 20−40 ppm region of the spectrum (including peak k) were also irradiated in 90% H_2O/10% D_2O (at pH 8 and 5.6) and 99.9% D_2O (data not shown). No NOEs are observed to signals i or j, and therefore, none of these three peaks are the His81 C$^{\epsilon 1}$H resonance, which must either be too broad to be observed or overlaps with another signal in the spectrum. Peak k does exhibit a weak NOE to peak g (the His40 C$^{\delta 2}$H), and thus, we can assign the former to the His40 C$^{\beta 1}$H resonance which is situated 3.71 Å from the C$^{\delta 2}$H and is 3.2 Å from the metal ion [in the (PA)Cu^{II} structure]. Peak k shows a strong NOE to a signal at 10.6 ppm (at 10 °C; data not shown), which we therefore assign to the His40 C$^{\beta 2}$H resonance.

Signal a, upon irradiation, shows a strong dipolar connectivity to peak e (see Figure 5C). The reverse NOE is observed upon irradiation of peak e (see Figure 5D). This clearly indicates that signals a and e are a geminal pair of protons. Peaks a and e also exhibit NOEs to peak d, which has an intensity equivalent to three protons and must therefore arise from a methyl group in the vicinity of the Ni(II) ion. The C$^{\epsilon}$H$_3$ moiety of the Met86 ligand is the only methyl group within 6 Å of the metal ion in the structure of

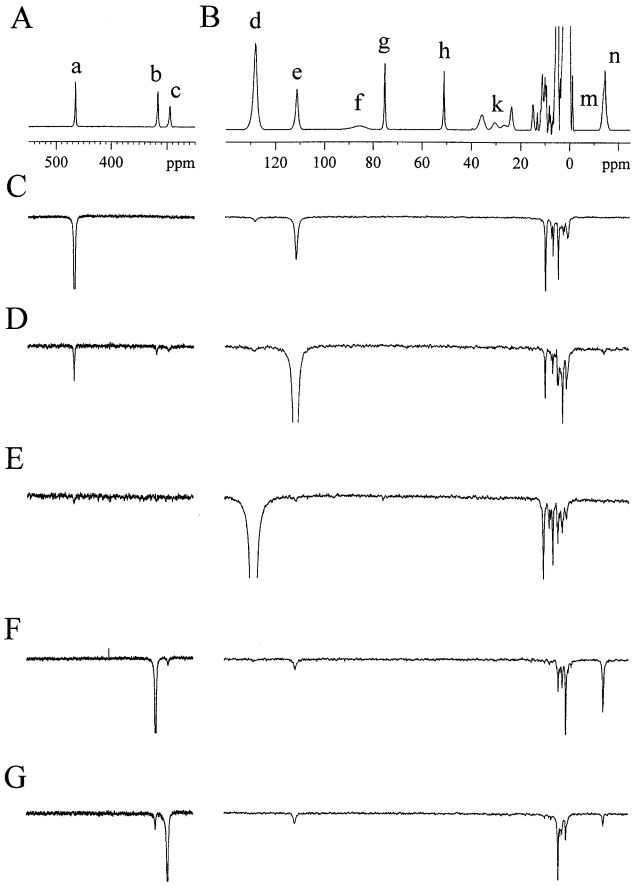

Figure 5. Reference (A and B) and difference (C−G) ^{1}H NMR spectra (300 MHz) of (PA)Ni^{II} corresponding to 1D NOE experiments performed in 10 mM phosphate buffer in 99.9% D_2O (10 °C) at pH* 8.0. In spectra C−G peaks a, e, d, b, and c, respectively, were irradiated.

(PA)Cu^{II} [the C$^{\epsilon}$ atom of Met86 is 3.5 Å from the Cu(II) ion]. Therefore, considering the relaxation properties of peak d and its large observed chemical shift (which is mainly Fermi contact in origin; vide infra), we conclude that it must belong to the C$^{\epsilon}$H$_3$ of the axial Met ligand. Furthermore, signal d exhibits a weak NOE to peak g (see Figure 5E) completely consistent with observed distance between the methyl group of Met86 and the His40 C$^{\delta 2}$H proton in the structure of (PA)Cu^{II} (vide infra). The irradiation of peak d results in the observation of the reverse NOEs to peaks a and e (see Figure 5E). This pattern of NOEs leads to the unambiguous assignment of peaks a and e as the C$^{\gamma}$H protons of the axial Met86 ligand.

Peaks b and c exhibit a strong dipolar connectivity (see Figures 5F and 5G) and thus belong to a geminal pair of protons. Irradiation of both peaks b and c leads to an NOE to peak e (a Met86 C$^{\gamma}$H proton). Additionally NOEs are observed between peaks b and c and peak n, with a much more intense NOE seen when peak b is irradiated. This pattern of NOEs is consistent with peaks b and c belonging to the C$^{\beta}$H protons of the Cys78 ligand. The NOE observed between both signals b and c and peak e identifies the latter as the C$^{\gamma 2}$H of Met86, which is situated 2.27 and 2.52 Å from the Cys78 C$^{\beta 1}$H and C$^{\beta 2}$H protons, respectively, in the (PA)Cu^{II} structure (the C$^{\gamma 1}$H of Met86 is situated 3.81 and 4.16 Å from the Cys78 C$^{\beta 1}$H and C$^{\beta 2}$H protons, respectively).

Table 3. Calculated[a] (Calcd) and Observed[b] (Obsd) NOE[c] Intensities for the Hyperfine-Shifted Resonances in the ^{1}H NMR Spectrum of Pseudoazurin

	peak to which NOE is observed																			
	a		b		c		d		e		g		h		i		j		n	
peak irradiated	calcd	obsd	calcd	obsd	calcd	obsd	calcd	obsd	calcd	obsd	calcd	obsd	calcd	obsd	calcd	obsd	calcd	obsd	calcd	obsd
a							0.3	1.1	16.8	19.3										
b					5.4	4.2	0.3	0.2	2.1	4.9									12.6	12.8
c			7.5	9.9					3.9	7.2									2.9	4.1
d	0.1	0.4	0.06	no[d]					0.3	0.5	0.1	0.3								
e	5.7	4.3	0.9	1.8	1.2	1.8	0.3	0.9											0.3	0.6
g							0.03	no									5.8	4.9		
h															3.8	2.6				
i													6.8	4.2						
j											6.0	3.1								
n			1.3	1.7	0.2	no			0.0 7	no										

[a] Using eq 1, a τ_r value of 1×10^{-8} s, the T_1 values and assignments listed in Table 2, and interproton distances derived from the structure of (PA)Cu^{II} (PDB accession code 1BQK with protons added in Insight II). [b] For (PA)Ni^{II} at 10 °C and 300 MHz. [c] The intensities of the NOEs are reported as percentages with the minus sign omitted. [d] Not observed due to an insufficient signal-to-noise ratio.

The irradiation of peak n did not result in the observation of any NOEs, except to peak b; thus, we assign peak n to the Cys78 C$^{\alpha}$H proton. The relative intensities of the NOEs between peaks b and c and peak n suggests that peak b belongs to the Cys78 C$^{\beta 2}$H, which is situated 2.36 Å from the C$^{\alpha}$H proton, whereas peak c arises from the Cys78 C$^{\beta 1}$H, which is slightly further from the C$^{\alpha}$H proton (3.02 Å).

The above assignments for the Cys and Met resonances are further confirmed by the observed weak NOE between peak b and signal d (see Figure 5F). This NOE is completely consistent (vide infra) with the observed interproton distances between the C$^{\beta 2}$H of Cys78 and the C$^{\epsilon}$H$_3$ group of Met86 in the structure of (PA)Cu^{II}.

An alternative assignment for peak n is that it could belong to the Met86 C$^{\beta 1}$H proton. The Cys78 C$^{\beta 1}$H is situated 2.16 Å from the Met86 C$^{\beta 1}$H, reasonably consistent (vide infra) with the strong NOE to peak n observed upon irradiation of peak b (this would lead to the opposite stereospecific assignment of the C$^{\beta}$H protons of Cys78). The corresponding NOE (between the ligand Cys C$^{\beta 1}$H and Met C$^{\beta 1}$H proton resonances) has been observed in paramagnetic NMR studies of other Ni(II) and Co(II) cupredoxins.[38,40,52,58] The Cys78 C$^{\beta 2}$H is 3.69 Å from the Met86 C$^{\beta 1}$H, which agrees with the much weaker NOE observed to peak n upon irradiation of peak c (but vide infra). The lack of any significant NOEs between peak n and other paramagnetic proton resonances (except signal b; data not shown) could indicate that peak m, which overlaps with signal n, arises from the Met86 C$^{\beta 2}$H proton (the NOE between such closely situated resonances in the spectrum would be impossible to observe). The lack of clear NOEs between the Met86 C$^{\gamma}$H protons (peaks a and e) and either peak m or n (a very weak NOE is observed between peaks e and n; see Figure 5D) would tend to indicate that these alternative assignments are less likely to be correct (vide infra).

The results of all of the 1D NOE difference experiments that have been carried out for (PA)Ni^{II} are listed in Table 3. Also included in this table are calculated NOE values determined using eq 1, a τ_r value of 1×10^{-8} s [as found for azurin,[82,83] a cupredoxin with a M_r similar to that of (PA)-Cu], the T_1 values and assignments listed in Table 2, and interproton distances derived from the structure of (PA)Cu^{II}. From the values listed in Table 3 we can see that the agreement between calculated and observed NOE intensities is qualitatively very good further confirming the correctness of the assignments that we have made. In particular the agreement of the observed and calculated values between peaks d and g and also peaks b and d is notable (vide supra). Furthermore, the conformity of the observed and calculated NOEs between peaks b and c and signal n confirms not only that peak n is the Cys C$^{\alpha}$H resonance but also that the correct stereospecific assignment of the Cys C$^{\beta}$H protons has been made. If signal n was the Met86 C$^{\beta 1}$H resonance (vide supra), then NOE intensities of 21.4% and 0.9% would be expected upon irradiation of signals b and c, respectively. Also noteworthy in Table 3 is the agreement of the observed and calculated NOE intensities to signal e upon irradiation of peaks b and c, which further confirms the correct stereospecific assignment of the Cys78 C$^{\beta}$H signals.

Effect of pH on the ^{1}H NMR Spectrum of (PA)Ni^{II}. In the diamagnetic region of the ^{1}H NMR spectrum of (PA)-Ni^{II} at pH 8.4 two singlets (actually unresolved doublets), which give rise to a TOCSY cross-peak, are observed at 8.04 and 7.36 ppm. These peaks are assigned as the imidazole ring protons of the noncoordinating His6 (the N$^{\delta}$ atom of this His is situated ~13.8 Å from the copper). The chemical shift values of both of these peaks are dependent on pH in the range ~8−5 with the peak at 8.04 ppm exhibiting the larger movements with changing pH (see Figure 6). This peak is thus assigned to the C$^{\epsilon 1}$H of His6, and that at 7.36 ppm arises from the C$^{\delta 2}$H proton. The dependence on pH of these two resonances (see Figure 6) can be fit to eq 2 giving pK_a values of 6.5.

In the paramagnetic ^{1}H NMR spectrum of (PA)Ni^{II} most of the hyperfine shifted resonances are slightly influenced by changing the pH value in the range 8.0 to 5.1 (see Figures 3A and 3B and Table 4). Plots of pH against chemical shift are shown in Figure 7A for the Met86 C$^{\gamma 1}$H resonance (peak a) and in Figure 7B for the Cys78 C$^{\beta}$H signals (peaks b and

(82) Kroes, S. J.; Canters, G. W.; Gilardi, G.; Van Hoek, A.; Visser, J. W. G. *Biophys. J.* **1998**, *75*, 2441−2450.

(83) Kalverda, A. P.; Ubbink, M.; Gilardi, G.; Wijmenga, S. S.; Crawford, A.; Jeuken, L. J. C.; Canters, G. W. *Biochemistry* **1999**, *38*, 12690−12697.

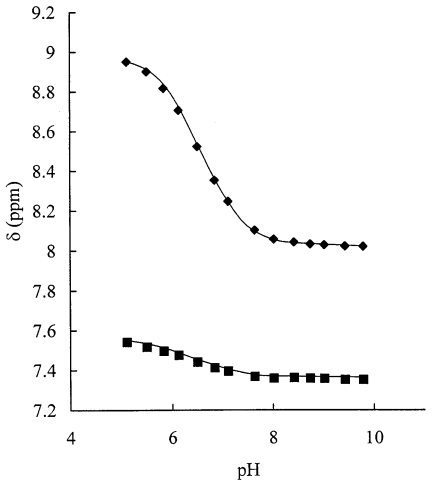

Figure 6. Dependence on pH of the chemical shift of the His6 $C^{\epsilon 1}H$ (◆) and $C^{\delta 2}H$ (■) resonances in the ^{1}H NMR spectrum of (PA)Ni^{II} in 10 mM phosphate (25 °C). The solid lines show the fit of the data to eq 2.

Table 4. Effect of pH on the Hyperfine-Shifted Resonances in the ^{1}H NMR Spectrum of (PA)Ni^{II} at 25 °C[a]

resonance	assignment	δ (ppm) at pH 5.1	δ (ppm) at pH 8.0	δ (ppm) at pH 10.8
a	Met86 $C^{\gamma 1}H$	429.0	432.5	424.5
b	Cys78 $C^{\beta 2}H$	297.6	296.6	295.5
c	Cys78 $C^{\beta 1}H$	270.8	274.0	264.8
d	Met86 $C^{\epsilon}H_3$	118.9	119.0	115.0
e	Met86 $C^{\gamma 2}H$	107.3	105.4	103.5
f	His40 $C^{\epsilon 1}H$	78.3	80.0	79.1
g	His40 $C^{\delta 2}H$	70.8	71.0	70.9
h	His81 $C^{\delta 2}H$	49.1	48.7	46.4
i	His81 $N^{\epsilon 2}H$	41.1		
j	His40 $N^{\epsilon 2}H$	38.1	38.5	
k	His40 $C^{\beta 1}H$	29.2	29.2	29.8
l		−11.7	−11.9	−11.4
m		−10.8	−12.8	−16.8
n	Cys78 $C^{\alpha}H$	−13.0	−13.6	−13.9

[a] Data recorded at 300 MHz in 90% H_2O/10% D_2O. Also included are the assignments that have been made.

c). Fits of the data in the pH range ~8−5, to eq 2, yield pK_a values of 6.4−6.5. Almost identical pK_a values are obtained from the analysis of the data for peaks e, g, h, j, m, and n (peaks d, k, and l shift very little in this pH range making precise fitting of the data difficult, peak f is very broad and its position is not easily measured precisely, and peak i is only observed at pH values below 5.8 at 25 °C).

$$\delta = (K_a\delta_H + [H^+]\delta_L)/(K_a + [H^+]) \quad (2)$$

The positions of most of the hyperfine-shifted resonances are also affected by raising the pH of (PA)Ni^{II} from 8.0 to 10.8 (see Figure 3B,C and Table 4), and in almost all cases the effects observed are greater than those seen upon lowering the pH value (see Figures 3 and 7 and Table 4). The dependence on pH of the positions of signals in this range can be divided into two groups. First there are those peaks which move in a continuous downfield direction as the pH is altered. Examples of such signals are the Met86 $C^{\gamma 1}H$ resonance (peak a) (see Figure 7A) and the Cys78 $C^{\beta 1}H$ (peak c) (see Figure 7B). Other peaks which behave in a similar manner are the Met86 $C^{\epsilon}H_3$ and $C^{\gamma 2}H$ resonances (peaks d and e, respectively), the His81 $C^{\delta 2}H$ signal (peak

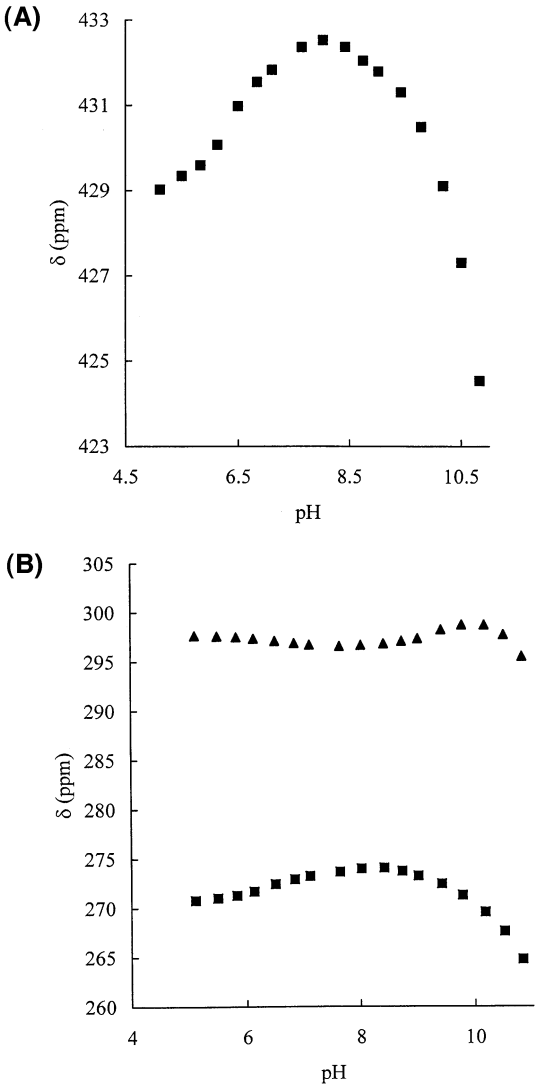

Figure 7. Dependence on pH (25 °C) of the chemical shift of the $C^{\gamma 1}H$ of Met86 (A) and the Cys78 $C^{\beta 1}H$ (■) and $C^{\beta 2}H$ (▲) protons (B) in the ^{1}H NMR spectrum of (PA)Ni^{II} in 10 mM phosphate buffer.

h), and peak m. Attempts to fit these data to eq 2 resulted in poor fits and pK_a values of 10.4 to 10.9. This large range of values is partly due to the incomplete nature of the titration curves for these peaks and also because of the instability of (PA)Ni^{II} at pH values above 10.5 (vide infra). The second group of signals are those which shift in one direction as the pH is raised from 8 to 10 and then above pH 10 begin to shift in the opposite direction. The pH dependence of the chemical shift of the Cys78 $C^{\beta 2}H$ (peak b) shown in Figure 7B demonstrates that this proton belongs in this category. Other peaks which behave in a similar manner are the His40 $C^{\delta 2}H$ (peak g) and peak l. The behavior of the latter group of signals indicates that the pH dependence of the active site structure of (PA)Ni^{II} in this pH range is affected by the deprotonation/protonation of more than one amino acid residue (see Discussion), and thus, we have not fit these data (fitting is also hampered by the incomplete nature of the titration curves). It should be noted that the chemical shift of the resonances which exhibit a continuous alteration in their position upon increasing pH are also affected by these two (or more) titrating surface amino acid residues (but in

this case the effects occur in the same direction). This could be another contributing factor to the large range of pK_a values and the poor nature of the fits observed (vide supra).

Discussion

UV/Vis Spectrum of (PA)Ni^{II}. The UV/vis spectrum of (PA)Ni^{II} is remarkably similar to those that have been published for other Ni(II)-substituted cupredoxins.[26,30,45,58,81] The positions and intensities of the bands observed for the Ni(II) forms of pseudoazurin, amicyanin, and azurin (three cupredoxins which possess axial Met ligands, although azurin has a second axially interacting ligand; see Figure 1) are shown in Table 1. From this comparison it is clear that the spectrum of (PA)Ni^{II} exhibits greater similarity to that of Ni(II) amicyanin than the azurin analogue. The LF transitions appear to be slightly more intense and red shifted (for some of these bands) in (PA)Ni^{II} and Ni(II) amicyanin than in the azurin derivative. This is consistent[24,45,81] with the crystal structures of the Cu(II) proteins, where the active sites of pseudoazurin and amicyanin both have distorted tetrahedral geometry whereas azurin has a trigonal bipyramidal arrangement (see Figure 1). The main LMCT band is blue shifted in the spectra of (PA)Ni^{II} and Ni(II) amicyanin as compared to the azurin derivative. [We have recently recorded UV/vis spectra of various Ni(II)-substituted plastocyanins, and in this cupredoxin the main LMCT band is at 410 nm.[84]] This can be attributed to the stronger interaction with the axial Met ligand in the former two proteins (see Figure 1).[30,45,58,81] Adjusting the pH of (PA)Ni^{II}, from 8.0, has very little effect on its visible spectrum. At pH values above 10.5, and below 5.0, (PA)Ni^{II} bleaches quite rapidly, due to the loss of Ni(II) from the active site. The absence of any pH dependence of the visible spectrum of (PA)Ni^{II} in the range 5.0−10.3 is in stark contrast to what we have previously observed for the Cu(II) protein. In this case either raising or lowering the pH value from around neutral has a significant effect on the relative intensity of the two main LMCT visible absorption bands (at 594 and 452 nm) of the protein.[68] At pH 8.0 the A_{452}/A_{594} ratio is 0.42 whereas at alkaline (>11.0) and low (<5.5) pH the ratio is 0.36.

^{1}H NMR Spectrum of (PA)Ni^{II}. The assigned ^{1}H NMR spectrum of (PA)Ni^{II} provides detailed structural information about the active site of this cupredoxin. The related cupredoxins amicyanin and azurin have been studied in their Ni(II) forms,[32,34,45,53,58] and it is on these three derivatives that we concentrate our comparisons [see Figure 1 for the active site structures of the three Cu(II) proteins]. The paramagnetic NMR data for the three Ni(II)-substituted proteins are shown in Table 5. The observed shifts (δ_{obs}) for the signals in the NMR spectrum of a paramagnetic molecule arise from three contributing factors shown as follows:

$$\delta_{obs} = \delta_{dia} + \delta_{pc} + \delta_{Fc} \quad (3)$$

Here δ_{dia} is the shift in an analogous diamagnetic system and δ_{pc} and δ_{Fc} are the pseudocontact (through space) and Fermi contact (through bond) contributions, respectively, to the isotropic shift. The δ_{dia} values are all usually in the range of 0−10 ppm in diamagnetic cupredoxins and thus are ignored here. The pseudocontact contribution to the isotropic shift arises from the magnetic anisotropy of the particular system. To calculate the contribution of δ_{pc} to the isotropic shifts requires the orientation and components of the magnetic susceptibility (χ) tensor to be calculated. In the Ni(II),[53] Co(II),[53] and Cu(II)[85] forms of azurin, the orientation of the magnetic susceptibility tensor has been found and the χ_{zz} axis is tilted approximately 20° from the Cu−O(Gly45) axial bond in all cases. In the studies on Ni(II) azurin the pseudocontact shifts were found to be relatively small (the maximum value is 17.0 ppm for the His46 C$^{\epsilon 1}$H proton).[53] In Co(II) azurin much larger dipolar contributions to the isotropic shifts are observed.[53] The smaller pseudocontact shifts in the Ni(II) protein are partly attributed to the presence of only two unpaired electrons, as compared to three in the case of Co(II). Furthermore, a smaller magnetic anisotropy exists in the Ni(II) derivative. We have not determined the orientation of the magnetic susceptibility tensor in (PA)Ni^{II}, and we assume that, as in azurin,[53] the isotropic shifts of most of the peaks are dominated by Fermi-contact contributions and thus provide detailed information about the metal−ligand interactions. Recently the magnetic susceptibility and the orientation of its main axes for Co(II) rusticyanin have been found to be very similar to those of Co(II) azurin.[60]

The most outstanding feature of the ^{1}H NMR spectrum of (PA)Ni^{II}, compared to the other proteins included in Table 5, is the hyperfine shifts of the Met86 C$^{\gamma}$H protons. The δ_{obs} of 432.5 ppm (at 25 °C) for the C$^{\gamma 1}$H proton is the largest value seen for any resonance in the paramagnetic ^{1}H NMR

Table 5. Observed Hyperfine Shifts (δ_{obs}) in the ^{1}H NMR Spectrum of (PA)Ni^{II} Compared with the δ_{obs} Values for the Corresponding Resonances in Ni(II) Amicyanin and Ni(II) Azurin[a]

		δ_{obs} (ppm)		Ni(II) azurin[e]		
ligand[b]	proton	(PA) Ni^{II} [c]	Ni(II) amicyanin[d]	δ_{obs} (ppm)	δ_{pc} (ppm)	δ_{Fc} (ppm)
His	H$^{\delta 2}$	71.0	72.6	57.2	−0.3	51.9
	H$^{\epsilon 2}$	38.5	38.3	35.0	2.0	21.5
Cys	H$^{\beta 1}$	274.0	296.0	187.0	1.1	182.8
	H$^{\beta 2}$	296.6	254.0	233.0	−9.8	239.5
His	H$^{\delta 2}$	48.7	58.3	64.3	1.6	55.9
	H$^{\epsilon 2}$	43.2[f]		51.5[g]	3.7	36.2
Met	H$^{\gamma 1}$	432.5	172.5	111.3	−2.7	112.5
	H$^{\gamma 2}$	105.4	30.2	0.6	−4.9	4.0
	C$^{\epsilon}$H$_3$	119.0	111.0	30.3	−0.1	30.4
Gly[h]	H$^{\alpha 1}$			69.5	−6.5	65.4
	H$^{\alpha 2}$			14.1	−5.9	−11.4

[a] Also included are the calculated pseudocontact (δ_{pc}) and Fermi contact (δ_{Fc}) shifts of the resonances in Ni(II) azurin. [b] From top to bottom, His40, Cys78, His81, and Met86 for pseudoazurin, His54, Cys93, His96, and Met99 for amicyanin, and His46, Cys112, His117, and Met121 for azurin. [c] Measured at 25 °C and pH 8.0. [d] For *Paracoccus versutus* amicyanin at 30 °C and pH 7.5.[58] [e] For *Pseudomonas aeruginosa* azurin at 45 °C and pH 7.5.[53] [f] Measured at pH 5.6 and 10 °C. [g] Not observed at pH values higher than 7. [h] Azurin residue Gly45. The corresponding residues in pseudoazurin and amicyanin are Gly39 and Pro53, whose backbone carbonyl groups are further away from the metal ion, and therefore, isotropically shifted resonances from this residue are not observed.

(84) Dennison, C.; Sato, K. Unpublished results.

(85) Coremans, J. W. A.; Poluektov, O. G.; Groenen, E. J. J.; Canters, G. W.; Nar, H.; Messerschmidt, A. *J. Am. Chem. Soc.* **1994**, *116*, 3097−3101.

spectrum of a Ni(II), or Co(II), cupredoxin. The δ_{Fc} values for these protons not only depends on the hyperfine coupling [which is directly related to the spin density on the thioether sulfur of the Met ligand and, thus, indicates the strength of the axial Ni(II)−S(Met86) bond] but also relies on the Ni(II)−S$^{\delta}$−C$^{\gamma}$−H$^{\gamma}$ dihedral angles. The δ_{Fc} values of the axial Met C$^{\gamma}$H protons in Ni(II) azurin are thought to exhibit a cosine squared dependence on the Ni(II)−S$^{\delta}$−C$^{\gamma}$−H$^{\gamma}$ dihedral angle.[53] The values for these dihedrals (the angle for the C$^{\gamma 1}$H proton is quoted first) in the Cu(II) proteins are −166.7 and 77.3° in azurin [these are the average values from the four molecules in the unit cell in the structure with the PDB accession code 4AZU, with the angles ranging from 74.1 to 80.3° for the C$^{\gamma 1}$H and from −160.4 to −175.0° for C$^{\gamma 2}$H protons, respectively],[12] −177.3 and 67.0° in amicyanin [again these are average values for the three molecules in the unit cell of the structure with the PDB accession code 1ID2],[11] and −169.6 and −50.5° in (PA)Cu^{II} [taken from the structure with the PDB accession code 1BQK].[8] It is interesting to note that the values in Ni(II) azurin[39,41] are very similar to those in the Cu(II) protein. [The average values for these dihedral angles in the structure of Ni(II) Trp48Met azurin with the PDB accession code 1NZR are −176.7 and 70.2° for the C$^{\gamma 1}$H and C$^{\gamma 2}$H protons, respectively.] The different Cu(II)−S$^{\delta}$−C$^{\gamma}$−H$^{\gamma 1}$ dihedral angles in the three proteins would be expected to have very little effect on the δ_{Fc} values. The differences in the angles for the C$^{\gamma 2}$H protons will be more significant and may contribute to the increase in the δ_{obs} value in the series azurin < amicyanin < pseudoazurin. The differences in the δ_{obs} values of the C$^{\gamma 1}$H proton in these three cupredoxins therefore must be due to an increase in the axial Ni(II)−S(Met) interaction according to the order pseudoazurin > amicyanin > azurin. Due to uncertainties concerning the dihedral angles in the Ni(II) proteins and also the presence of dipolar ligand-centered effects (which detract from a quantitative correlation between these dihedrals and δ_{Fc} values), it has been proposed[60] that a more reliable estimate of the strength of the axial bond is obtained from an average of the δ_{obs} values for the two Met C$^{\gamma}$H protons ($\delta_{\gamma,av}$). The $\delta_{\gamma,av}$ values are 269, 101, and 56 ppm for Ni(II)-substituted pseudoazurin, amicyanin, and azurin, respectively, giving rise to relative strengths of the Ni(II)−S(Met) bond in the three proteins of 1:1.8:4.8 for azurin:amicyanin:pseudoazurin. This demonstrates a much stronger axial interaction in the case of (PA)Ni^{II} consistent with the Cu(II)−S(Met) bond lengths of 2.71,[8] 2.84,[11] and 3.11 Å[12] observed in the crystal structures of pseudoazurin, amicyanin, and azurin, respectively. This much stronger axial interaction in (PA)Ni^{II} is also consistent with the type 1 rhombic properties of (PA)Cu^{II} as compared to the type 1 axial sites of Cu(II) amicyanin and azurin. In the case of the paramagnetic NMR spectrum of (PA)Cu^{II},[68] only one of the Met C$^{\gamma}$H protons is observed. It was assumed that the second resonance is not shifted outside of the diamagnetic envelope, but in light of the data on the Ni(II) protein it may be that this resonance exhibits a sizable Fermi-contact shift but is too broad to be directly observed.

The strength of the axial M(II)−S(Met) bond also influences the Fermi contact shift of the C$^{\epsilon}$H$_3$ group of this coordinated residue.[38,40,52,53,58,60] This feature is free from an angular dependence, and for the Ni(II) proteins listed in Table 5, the δ_{obs} values of this resonance (119, 111, and 30.3 ppm for Ni(II) pseudoazurin, amicyanin,[58] and azurin,[53] respectively) follow the same pattern as that for $\delta_{\gamma,av}$ (vide supra). The only discrepancy is the size of the difference between the values for pseudoazurin and amicyanin. Further studies are currently underway to try to understand this inconsistency.

The isotropic shift of the ligating Cys C$^{\beta}$H protons in paramagnetic NMR studies provides detailed information about the M(II)−S(Cys) bond strength in cupredoxins. The δ_{Fc} value of the Cys C$^{\beta}$H protons is dependent on the M(II)−S$^{\delta}$−C$^{\beta}$−H$^{\beta}$ dihedral angles. These angles are very similar in all three Cu(II) proteins. [The average values for these dihedral angles are −48.9 (H$^{\beta 1}$) and 66.8° (H$^{\beta 2}$), −47.4 and 64.2°, and −47.0 and 68.7° in azurin,[12] amicyanin,[11] and (PA)Cu^{II},[8] respectively.] An approach which has been adopted, when using the observed shifts of these protons as an indicator of the strength of the M(II)−S(Cys) interaction, has been to take an average value for the two signals ($\delta_{\beta,av}$), which is less sensitive to the orientation of the side chain of this residue.[49,60] The $\delta_{\beta,av}$ values are 210, 275, and 285 ppm in Ni(II) azurin,[53] amicyanin,[58] and pseudoazurin, respectively. This indicates similarities in this interaction between pseudoazurin and amicyanin and a weaker bond in the azurin derivative. Thus, it would appear that the increased axial interaction between Ni(II) and the thioether sulfur of Met86 in pseudoazurin does not weaken the bond with the thiolate sulfur of the Cys78 ligand. The small $\delta_{\beta,av}$ value for the Cys C$^{\beta}$H protons in Ni(II) azurin is probably a consequence of the two axially interacting amino acid residues at its trigonal bipyramidal active site (see Figure 1).

In the case of Cu(II) cupredoxins the Cys C$^{\beta}$H protons are too broad to be directly observed. However, an approach using blind saturation transfer experiments, on mixtures of the Cu(II) and Cu(I) proteins, has allowed the C$^{\beta}$H protons of the Cys ligand to be indirectly observed and assigned.[63,65,66] These resonances are found at 650 and 489 ppm in spinach plastocyanin,[63] 614 and 517 ppm in *Synechocystis* PCC6803 plastocyanin,[66] 850 and 800 ppm in azurin,[65] and 450 and 375 ppm in cucumber stellacyanin.[65] Despite the Cu(II) ion possessing only one unpaired electron, as compared to two for tetrahedral Ni(II), the shifts experienced by these protons in the Cu(II) proteins are considerably larger. This indicates greater unpaired spin density on the Cys C$^{\beta}$H protons in the Cu(II) proteins than that observed in the Ni(II)- [and also Co(II)-] substituted proteins.

The shifts observed for the imidazole ring protons of the two histidine ligands in (PA)Ni^{II} are very similar to those observed for the other Ni(II)-substituted proteins listed in Table 5. This indicates close similarities in these interactions in the different cupredoxins. A similar conclusion has been drawn from paramagnetic NMR studies of the Cu(II) proteins.[62,65,68]

Effect of pH on the ^{1}H NMR Spectrum of (PA)Ni^{II}. The imidazole ring protons of His6, in the diamagnetic region of the spectrum of (PA)Ni^{II}, shift in the pH range 9−5 (see Figure 6) giving rise to a pK_a of 6.5. This value is identical to the pK_a determined for His6 in (PA)Cu^{II} and is lower than the value for (PA)Cu^{I} (7.1).[68] This is consistent with the pK_a of His6 being influenced by the charge at the active site.

Both lowering and increasing the pH from 8.0 influences the paramagnetic ^{1}H NMR spectrum of (PA)Ni^{II}. This indicates that the protonation/deprotonation of amino acid residues relatively distant from the active site (as the observed effects are quite small) can influence the structure of the metal center. In both cases (lowering and raising the pH) the paramagnetic signals shift as the pH is altered, and thus, both processes are in the fast-exchange regime. The influence of pH on the paramagnetic NMR spectrum of the Cu(II) protein has recently been studied.[64,68] In the Cu(II) protein we have found that a similar active site modification is observed upon lowering and increasing the pH value. This change in structure involves the movement of the copper ion away from the axial Met86 ligand toward the plane of the three equatorial ligands at extremes of pH. The effect observed at acidic pH values has been attributed to His6 (pK_a $\sim$ 6.5), while that at alkaline pH has been attributed to one or more of the Lys residues which surround the hydrophobic patch of (PA)Cu through which the ligand His81 protrudes. In (PA)Ni^{II} the effects seen in the paramagnetic ^{1}H NMR spectrum upon lowering the pH (see Figures 3A,B and 7A,B and Table 4) all give rise to pK_a values of approximately 6.5. Thus, we can assign this effect to the protonation of His6 which, as in the copper protein, has an influence on the active site structure of (PA)Ni^{II}. The $\delta_{\gamma,av}$ (Met86) value decreases from 269.0 ppm at pH 8.0 to 268.2 ppm at pH 5.1, while the $\delta_{\beta,av}$ (Cys78) value also decreases from 285.3 ppm at pH 8.0 to 284.2 ppm at pH 5.1. Alterations in the chemical shift values of other hyperfine-shifted resonances, including the Met86 C$^{\epsilon}$H$_3$ signal and peaks arising from the two His ligands, are very small. The protonation of His6 has a much more limited effect on the active site structure of (PA)Ni^{II} than is the case in the Cu(II) protein. [In (PA)-Cu^{II} the δ_{Fc} value of one of the Met86 C$^{\gamma}$H protons decreases by 20% upon protonation of His6.] Furthermore, it appears that the effect of protonation of this surface residue on the active site structure is not concerted as in the case of the copper protein, and the observed effects are consistent with small changes in bond distances or angles (approximately a few tenths of an angstrom or a few degrees) around the nickel center as a result of the protonation of His6.

Increasing the pH from 8.0 has a more dramatic effect (than the protonation of His6) on the paramagnetic ^{1}H NMR spectrum of (PA)Ni^{II} (see Figures 3 and 7A,B and Table 4), and values of 264 and 280.2 ppm are obtained for $\delta_{\gamma,av}$ and $\delta_{\beta,av}$, respectively, at pH 10.8. Adjustment of the pH in this range also has quite significant effects on the δ_{obs} values of the Met86 C$^{\epsilon}$H$_3$ signal, the His81 C$^{\delta 2}$H resonance, and peak m. In all cases, except peak m, a decrease in the magnitude of δ_{obs} is seen at pH 10.8, as compared to pH 8.0, indicating that all of the Ni−ligand interactions are diminished at high pH (alterations in the orientation of ligating amino acid residues cannot be discounted as also contributing to the observed effects). In comparison to studies on (PA)Cu^{II} the alkaline transition also has a much more limited effect on the active site structure in (PA)Ni^{II}.

The alkaline transition in (PA)Cu^{II} has previously[64] been assigned to one or more of the surface Lys residues close to the active site. In particular Lys38, which is situated close to the exposed His81 ligand, and Lys77, which is adjacent to the Cys78 ligand, have been implicated. The behavior of certain resonances (peaks b, g, and l) in (PA)Ni^{II} upon increasing pH, which shift in one direction up to pH 10 and then shift in the opposite direction at more alkaline pH values, is particularly interesting in this respect. These results indicate that the alkaline transition arises from more than one surface exposed Lys residue, which possess different pK_a values. [The N$^{\zeta}$ atoms of Lys38 and Lys77 are situated 13.5 and 11.2 Å from the Cu(II) ion in the (PA)Cu^{II} structure.] Thus, it would appear that the titration of both Lys38 and Lys77 has an effect on the active site structure of the protein. Further studies on site-directed mutants of pseudoazurin are currently underway to investigate the exact cause of the alkaline transition in more detail.

Conclusions

The hyperfine-shifted signals in the paramagnetic ^{1}H NMR spectrum of (PA)Ni^{II} have been assigned and provide a detailed insight into the electronic structure of the active site of this cupredoxin. The relative strength of the axial Ni(II)−S(Met) bond is indicated by the remarkably large shift of the C$^{\gamma}$H protons of this ligand, as compared to other Ni(II)-substituted cupredoxins. The stronger axial interaction in the case of (PA)Ni^{II} does not result in a weakening of the Ni(II)−S(Cys) bond. In fact the $\delta_{\beta,av}$ value for (PA)Ni^{II} is the largest seen for a Ni(II) cupredoxin. The influence of pH on the paramagnetic NMR spectrum of (PA)Ni^{II} highlights that the acid (His6) and alkaline (Lys38 and Lys77) transitions influence the structure of the active site. However, the observed effects in the Ni(II) protein are much smaller than in the native Cu(II) protein.

Acknowledgment. We thank the University of Newcastle upon Tyne and the Royal Society for funding, the CVCP for an ORS award, and the EPSRC for a grant to purchase the NMR spectrometer. We thank Prof. T. Kohzuma (Ibaraki University, Ibaraki, Japan) for providing the bacterial strain of *A. cycloclastes* and Prof. A. Harriman and A. Amini (University of Newcastle upon Tyne) for access to and assistance with Insight II.

IC020303P